NASA Technical Paper 1397

Design and Analysis of an Active Jet Control System for Helicopter Sling Loads

Mark D. Pardue and J. D. Shaughnessy

JANUARY 1979

NASA

NASA Technical Paper 1397

Design and Analysis of an Active Jet Control System for Helicopter Sling Loads

Mark D. Pardue
Old Dominion University
Norfolk, Virginia

and

J. D. Shaughnessy
Langley Research Center
Hampton, Virginia

National Aeronautics
and Space Administration

**Scientific and Technical
Information Office**

1979

SUMMARY

An active jet control system for stabilizing the swinging motion of helicopter external sling loads in hover (and forward flight) is described. A velocity feedback control law is obtained by using classical control theory. A nondimensional analysis is performed to give a simple chart for determining the appropriate value of feedback gain as a function of cable length, sling length, and load parameters to provide theoretical damping ratios of 0.7. The sensitivity to parameter changes was studied, and a ±10-percent change in parameters was found to affect system performance only slightly. Implementation of the control scheme in a nonlinear simulation produced damping ratios equal to or greater than those calculated. A limited number of piloted flights in a visual simulator indicated a significant reduction in load swinging in the transition to hover, and thus the pilot was able to concentrate on load altitude and position control.

INTRODUCTION

There has been increasing activity in the area of helicopter sling-load work over the past few years. This involves pickup, transportation, and placement of various sizes, shapes, and weights of loads for different makes and models of helicopters and for various lengths and arrangements of cables and load slings. Loads vary in mass up to 14 000 kg and include pylons, air conditioners, sports grandstands, and construction materials.

Load stabilization and control is a complicated procedure for the helicopter pilot because the helicopter must be moved above the load in such a way as to minimize swinging of the load. The complicated maneuvering by the pilot promotes the probability of pilot error and accident. Reference 1 indicates that pilot error was a contributing factor in 63 percent of all sling load accidents during the period 1968 to 1974. Decreasing pilot workload by lessening corrective maneuvering would have a positive effect on accident reduction.

Several control systems that dampen swinging of the load and thus reduce pilot workload have been studied. Research control systems have been developed to move the helicopter with respect to the load in order to dampen swinging of aerodynamically stable loads (refs. 2 to 4). These are complex subsystems added to the automatic flight control system of the aircraft and are especially designed for each specific model of helicopter (ref. 5).

Many of the sling loads carried are aerodynamically unstable, such as the 2.4-m by 2.4-m by 6.1-m cargo container used by the U.S. Army. Automatic control systems of the type mentioned above cannot control these loads well in forward flight (ref. 6); therefore, several mechanical control systems have been developed to stabilize them. A system using aerodynamic fins placed at the load was studied and showed moderate damping in cruise flight, but little damping at low velocities (ref. 7). The system made use of a tandem cable arrangement. Both position and velocity were fed back to stabilize the load. The Cornell

Aeronautical Laboratory made a theoretical study of an active winch control system which used three cables and controllable winches (ref. 8). Accelerometers and rate gyros along with filters were used to measure the variables needed in the control system, which provided moderate damping in hover and forward flight. An active arms control system developed by the U.S. Army gave moderate damping in flight and hover (refs. 5 and 9) by means of a tandem cable arrangement and controllable mechanical arms through which the cables were attached to the helicopter. Control system variables were measured by using synchros.

The subject of this report is the control system shown in figure 1. This system was suggested by NASA test pilot Kenneth R. Yenni and NASA aerospace technologist J. D. Shaughnessy of the Langley Research Center. Four reaction jets aligned orthogonally with each other in a plane normal to the cable provide control forces.

This control system scheme is potentially superior to others developed, for several reasons. The system utilizes a single cable, which is the most common type of suspension for sling loads, and it uses no special load slings. Although a tandem cable arrangement can reduce load yawing oscillations, it is prone to longitudinal swinging, increases weight, and increases load hookup time (ref. 10). The active jet control system (AJS) is expected to provide good damping both in hover and in flight, whereas other systems provide relatively low or moderate damping in hover, which is the most accident-prone stage in helicopter sling-load work (ref. 1). Also, the helicopter does not need an automatic flight control system or a stability augmentation system to implement the AJS. The AJS should decouple load control and helicopter control by placing the load control force below the helicopter and independently of the helicopter. This feature is an improvement. By decoupling the load and helicopter controls, the helicopter pilot can control just the helicopter without interference from the load control system, and thus pilot workload is reduced.

Implementation of the AJS concept requires some type of thrust-producing mechanism. Figure 1 shows one concept of using high-pressure air generated by the helicopter power plant. The helicopter relative yaw angle of the jet system must be continuously determined, and certain other linear motions must be measured.

Problems associated with this type of system include the possibility that the jets used for the control force might remain on after the load has been released. The load cable could then be thrust up into the rotor and an accident would result. There would also be difficulties in measuring the relative motions of the load with respect to the helicopter.

This report develops and analyzes a longitudinal control law for the control system strategy described above and provides gains applicable to various helicopters, loads, and single-cable suspension systems. The control law developed should be equally applicable to the lateral motions.

For the control system design, the load is modeled by means of rigid-body equations of motion and small-angle approximations in the vertical plane. Cable vibrations are not considered. A transfer function of the relative velocity of the control point versus the control force is obtained, and

feedback control theory is used to stabilize the system and provide desirable damping characteristics.

The mathematical model of the control system is nondimensionalized and the effects of varying the nondimensional parameters (combinations of cable length, sling length, and radius or gyration) are presented. Graphs are presented for different loads and cable assemblies giving feedback gain required to provide good damping for different values of the nondimensional parameters. This information enables one to implement the AJS on different helicopters, carrying various loads and using various single-cable assemblies.

The implementation and results of the AJS in a helicopter sling-load simulation are presented. This is a digital computer simulation for the full flight envelope of a single-rotor helicopter transporting a sling load. The control system design is first simulated using nominal parameter values. Then the parameters are allowed to vary ±10 percent to represent the parameter estimation error that one would expect to encounter in normal helicopter sling-load operations. Performance of the AJS is presented through time histories.

The information in this paper is largely based on a thesis submitted by Mark D. Pardue in partial fulfillment of the requirements for the degree Master of Engineering, Old Dominion University, Norfolk, Virginia, May 1977.

SYMBOLS

a	acceleration of control point, m/s^2
$A(s)$	Laplace transform of a
F	control force, N
$F(s)$	Laplace transform of F
$\hat{F}(\hat{s})$	nondimensional $F(s)$, $\frac{F(s)}{mg}$
g	acceleration of gravity, 9.802 m/s^2
$G(s)$	load-position transfer function
I	inertia of the load, $kg\text{-}m^2$
k	radius of gyration of the load, m
K_a	acceleration feedback gain, $N\text{-}s^2/m$
K_p	position feedback gain, N/m
K_v	velocity feedback gain, N-s/m

$\hat{K}_v$	nondimensional velocity feedback gain, $\frac{K_v(\ell_1 + \ell_2)}{mg\sqrt{\ell_1/g}}$
ℓ_1	length of load cable, m
ℓ_2	length of load sling, m
m	mass of the load, kg
p_1, p_2	poles of transfer function
s	Laplace variable, $s = \sigma + j\omega$, s^{-1}
$\hat{s}$	nondimensional s, $s\sqrt{\ell_1/g}$
T	jet thrust, N
v	relative velocity of control point with respect to the helicopter, m/s
V(s)	Laplace transform of v
$\hat{V}(\hat{s})$	nondimensional V(s), $\frac{V(s)\sqrt{\ell_1/g}}{\ell_1 + \ell_2}$
x,y	longitudinal and lateral displacements of control point with respect to cable attachment point at the helicopter, m
X(s)	Laplace transform of x
x_1	displacement of load center of gravity with respect to cable attachment point at the helicopter, m
$X_1(s)$	Laplace transform of x_1
z_1, z_2, z_3	zeros of transfer function
α_1	nondimensional parameter, ℓ_1/ℓ_2
α_2	nondimensional parameter, $\ell_1\ell_2/k^2$
ζ	controlled system damping ratio
θ	load attitude, rad
$\theta(s)$	Laplace transform of θ

Subscripts:

x,y	component in load x- or y-direction

CONTROL LAW DEVELOPMENT

In this section the analysis and the development of the control system scheme shown in figure 1 are presented. The system to be controlled is first dynamically modeled. Then, through classical root-locus methods, the control law for this control system is defined.

Dynamic Model of a Sling Load

The dynamic system to be controlled is modeled as a double pendulum, as shown in figure 2. The cable attachment point at the helicopter is represented by point B; the point at which the control force is applied - in this case jet thrust - by point A. It is desired to stop load movement with respect to the helicopter. The model assumes that all members are rigid with two degrees of freedom. Small-angle approximations are used in the vertical plane. These approximations are valid because the amount of swing in relation to the cable length is expected to be small, since the control system should dampen the swinging motion of the load and not allow the swing to become large. Aerodynamic forces on the load are not modeled. The control force is assumed to be linearly proportional to the control signal. The linearized dynamic equations for the system shown in figure 2 are given in the appendix as

$$I\ddot{\theta} = -\left[x_1 + (\ell_1 + \ell_2)\theta\right] mg \frac{\ell_2}{\ell_1} + F\ell_2 \tag{1}$$

and

$$m\ddot{x}_1 = -(x_1 + \ell_2\theta)\frac{mg}{\ell_1} + F \tag{2}$$

The load-position transfer function is derived in the appendix and is given as

$$\frac{X(s)}{F(s)} = \frac{\left(\frac{k^2 + \ell_2^2}{mk^2}\right)\left(s^2 + \frac{\ell_2 g}{k^2 + \ell_2^2}\right)}{s^4 + \frac{\left[\ell_2(\ell_1 + \ell_2) + k^2\right]gs^2}{k^2\ell_1} + \frac{g^2\ell_2}{k^2\ell_1}} = G(s) \tag{3}$$

Design of Control System Scheme by Root Locus

Examination of the denominator of equation (3) shows that the uncontrolled system has two undamped oscillatory modes of motion. A low-frequency mode

associated with open-loop poles p_1 and p_1^* shown in figure 3 corresponds to the pendulum motion of the entire double pendulum. A high-frequency mode associated with open-loop poles p_2 and p_2^* in figure 3 corresponds to the rocking motion of the lower pendulum.

Three feedback schemes are considered next, and on the basis of their root-locus plots, one system is chosen to be studied further.

Feeding back position x through a gain $-K_p$, as shown in figure 4, yields the root locus shown in figure 3 for the following set of nominal parameters:

$$\ell_1 = 30.5 \text{ m}$$

$$\ell_2 = 6.1 \text{ m}$$

$$m = 4536 \text{ kg}$$

$$k^2 = 3.6 \text{ m}^2$$

This feedback system is marginally stable because it has roots lying on the imaginary axis. This is unsatisfactory because no damping is achieved.

Note that

$$V(s) = s\,X(s) - x(0)$$

Therefore, from equation (3),

$$\frac{V(s)}{F(s)} = s\,G(s) \tag{4}$$

Feeding back relative velocity through a gain $-K_v$, as shown in figure 5, yields the stable root locus shown in figure 6.

It is seen in figure 6 that there are two possible root-locus configurations, depending on pole and zero placement, but both configurations are asymptotically stable for $0 < K_v < \infty$.

From equations (3) and (4), the acceleration transfer function is

$$\frac{A(s)}{F(s)} = s^2\,G(s)$$

Feeding back acceleration a through a gain $-K_a$, as shown in figure 7, yields the marginally stable root locus shown in figure 8, which is unacceptable. Adding a lead compensator of the form $\frac{s + b}{s + c}$ (where $c > b$), as shown in figure 9, yields the stable root locus shown in figure 10 but does not provide as significant damping of the pendulum-mode roots as that obtained using velocity feedback; nor does adding this lead compensator cascaded with the velocity feedback gain K_v improve the damping in the velocity feedback system. Controlling velocity accomplishes the objective of damping the swinging of the load; therefore, the velocity feedback control system shown in figure 5 is the design which was selected to be investigated, and thus the control law is $F = -K_v v$.

FEEDBACK GAINS FOR VARIATIONS IN PARAMETERS

The placement of the open-loop poles and zeros of the velocity feedback control system affects the shape of the root locus. This placement is affected by changes in the length parameters ℓ_1 and ℓ_2 and the radius of gyration k. By using nondimensional combinations of ℓ_1, ℓ_2, and k and algebraic manipulation, it is possible to reduce the number of independent parameters affecting the placement of the open-loop poles and zeros. In this section, nondimensional parameters are obtained and then varied to obtain values of feedback gain for the best damping available for each configuration.

Nondimensionalizing $V(s)/F(s)$

When both the numerator and denominator of equation (4) are multiplied by $(\ell_1/g)^2$ and the result is simplified to obtain nondimensional terms, the transfer function $V(s)/F(s)$ becomes

$$\frac{V(s)}{F(s)} = \frac{\left(\frac{\ell_1}{mg}\right)\left(\frac{\ell_2}{\ell_1}\right)\left(\frac{\ell_1}{\ell_2} + \frac{\ell_1\ell_2}{k^2}\right)s\left[s^2\left(\frac{\ell_1}{g}\right) + \frac{1}{\frac{k^2}{\ell_1\ell_2} + \frac{\ell_2}{\ell_1}}\right]}{s^4\left(\frac{\ell_1^2}{g^2}\right) + \left[\frac{\ell_1\ell_2}{k^2}\left(\frac{\ell_2}{\ell_1} + 1\right) + 1\right]s^2\left(\frac{\ell_1}{g}\right) + \frac{\ell_1\ell_2}{k^2}} \tag{5}$$

By letting $\hat{V}(\hat{s}) = \frac{V(s)\sqrt{\ell_1/g}}{\ell_1 + \ell_2}$, $\hat{F}(\hat{s}) = \frac{F(s)}{mg}$, and $\hat{s} = s\sqrt{\ell_1/g}$, all of which are nondimensional, the following equations are obtained:

$$\frac{\hat{V}(\hat{s})}{\hat{F}(\hat{s})} = \frac{V(s)}{F(s)} \frac{mg\sqrt{\ell_1/g}}{\ell_1 + \ell_2} \tag{6}$$

or

$$\frac{\hat{V}(\hat{s})}{\hat{F}(\hat{s})} = \frac{\left(\dfrac{1}{\dfrac{\ell_1}{\ell_2} + 1}\right)\left(\dfrac{\ell_1}{\ell_2} + \dfrac{\ell_1\ell_2}{k^2}\right)\hat{s}\left(\hat{s}^2 + \dfrac{1}{\dfrac{k^2}{\ell_1\ell_2} + \dfrac{\ell_2}{\ell_1}}\right)}{\hat{s}^4 + \left[\left(\dfrac{\ell_1\ell_2}{k^2}\right)\left(\dfrac{\ell_2}{\ell_1} + 1\right) + 1\right]\hat{s}^2 + \dfrac{\ell_1\ell_2}{k^2}} = \frac{\left(\dfrac{\alpha_1 + \alpha_2}{\alpha_1 + 1}\right)\hat{s}\left(\hat{s}^2 + \dfrac{1}{\dfrac{1}{\alpha_2} + \dfrac{1}{\alpha_1}}\right)}{\hat{s}^4 + \left[\alpha_2(1 + \alpha_1) + 1\right]s^2 + \alpha_2} \tag{7}$$

where $\alpha_1 = \ell_1/\ell_2$ and $\alpha_2 = \ell_1\ell_2/k^2$.

It is seen that in equation (7) only two parameters affect the placement of open-loop poles and zeros in the $\hat{s}$-plane. These two, α_1 and α_2, are both nondimensional. The nondimensionalized transfer function $\hat{V}(\hat{s})/\hat{F}(\hat{s})$ can now be analyzed just as the original transfer function $V(s)/F(s)$, and only the variations of the two nondimensional parameters need to be studied. The control law may now be defined from equation (6) as $F = -K_v v$, where

$$K_v = \hat{K}_v \frac{mg\sqrt{\ell_1/g}}{\ell_1 + \ell_2} \tag{8}$$

Obtaining Feedback Gains for Variations of Nondimensional Parameters

Referring to figure 6, there are two possible root-locus configurations possible. The root locus shown at the top of figure 6 corresponds to the shaded region in figure 11, where a damping ratio ζ of 0.7 is possible. The root locus at the bottom of figure 6 corresponds to the unshaded region in figure 11, where only damping ratios smaller than 0.7 are possible. After generating root loci for variations of the two nondimensional parameters, the feedback gain $\hat{K}_v$ required for the highest damping possible for each configuration, up to $\zeta = 0.7$, was recorded. This information is graphed in figure 11.

From figure 11, it is seen that for $\ell_1\ell_2/k^2 \geq 1.5$ and $\ell_1/\ell_2 > 5$, damping ratios of 0.7 are possible. Cable lengths much larger than sling lengths are typical in sling-load work, as are cable lengths of 30 to 70 m. Because longer

sling lengths, greater than 4 to 6 m, have been shown to increase load instability (ref. 6), $\ell_1/\ell_2 \geq 5$ is a normal operating condition. The condition $\ell_1\ell_2/k^2 \geq 1.5$ is also a normal operating condition, except for combinations of extremely large loads suspended on small cables and slings. For example, a large 6.1-m by 6.1-m by 2.4-m load might typically have $k^2 = 6.2$ m and $\ell_1\ell_2 \geq 9.3$ m^2. This yields $\ell_1\ell_2/k^2 \geq 1.5$. Thus, it is seen that the normal operating conditions of sling-load work lie in the shaded region of figure 11, where damping of 0.7 is possible.

The set of curves in figure 11 allows the velocity feedback control system to be used for a wide range of operating parameters. When a set of operating parameters has been chosen, the nondimensional parameters ℓ_1/ℓ_2 and $\ell_1\ell_2/k^2$ are calculated. The nondimensional feedback gain $\hat{K}_V$ can then be determined from the family of curves in figure 11. Finally, the actual controller gain to be used K_V is calculated from equation (8). The damping ratio of the two complex-conjugate roots associated with the low-frequency pendulum mode of motion of the system is also presented in the graph in figure 11. The availability of high damping over a wide range of normal operating conditions shows the working feasibility of the orginal control strategy.

SIMULATION RESULTS

The active jet control system (AJS) with relative velocity feedback was implemented in a piloted helicopter sling-load simulation. The simulation was used to verify the feedback control performance, examine the effect of typical parameter variations, and obtain pilot opinions from a brief investigation.

Description of Simulation

The simulation used in this report is described in reference 11. The mathematical model for the helicopter and the load has nonlinear equations of motion with nonlinear aerodynamics. Modified Bailey rotor theory is used to model the main and tail rotors. The equations of motion for both the helicopter and load are written with respect to a flat, nonrotating Earth. The dimensions and weight of the load are variable. The load cable and cable stretch are modeled as a spring, and the cable length is variable. The atmosphere is modeled by using the standard atmosphere. Hover, forward flight, rearward flight, turns, and all other practical regimes of flight are possible, and any practical flight condition can be initially set into the simulation.

The helicopter control system is modeled with actuator dynamics and pilot inputs provided. An automatic flight control system is included for the purpose of stabilizing the helicopter during nonpiloted tests of the AJS. The automatic flight control system is needed because the basic helicopter is unstable. The AJS is independent of the automatic flight control system. The cockpit, which is connected to the real-time digital computer, contains complete pilot controls for a helicopter. The left and right pedals, cyclic stick, and collective stick are all linked to the computer through analog-to-digital converters. There is a visual landing display scene in the cockpit which is a

color display of the outside world as seen from the cockpit. There is also a computer-generated scene of the load as seen by the pilot looking down at the load. Standard flight instruments are provided in the cockpit.

Implementation of Control System in Simulation - Examples

The AJS was implemented in this simulation by feeding back the relative velocity of the control point calculated in the simulation computer program. This velocity signal is then multiplied by the control gain to give the control force, which is the thrust of the jets.

Two examples were considered for validation of the simulation. First, the following set of typical parameters were used: $\ell_1 = 30.5$ m, $\ell_2 = 6.1$ m, and a 2.4-m by 6.1-m by 6.1-m, 4536-kg load. This yields $\ell_1/\ell_2 = 5$ and $\ell_1\ell_2/k^2 = 51.7$. Thus, it is seen that this operating point lies in the shaded region of figure 11, where $\zeta = 0.7$ is possible and K_v is determined to be 4069 N-s/m. The second example has $\ell_1 = 6.1$ m, $\ell_2 = 6.1$ m, and a 6.1-m by 6.1-m by 6.1-m, 454-kg load. For this second example $\ell_1/\ell_2 = 1$ and $\ell_1\ell_2/k^2 = 6$; this condition lies in the unshaded region in figure 11. From figure 11 and equation (8), $K_v = 926.1$ N-s/m, and a calculated damping ratio of only 0.17 is possible. These parameter values are not considered normal operating conditions.

Figures 12 and 13 show the calculated migration of the roots of the pendulum mode of motion of the sling load with the AJS implemented, as the parameters are varied for the two examples. Weight, cable length, and sling length are the only parameters which affect the roots. Varying the inertia of the load has negligible effect. When the parameters and the feedback gain were varied ±10 percent, the calculated damping ratio of the pendulum-mode roots for example 1 varied from 0.57 to 0.78, with 0.70 at the design point; the damping ratio for example 2 varied from 0.14 to 0.20, with 0.17 at the design point.

The AJS was implemented on the helicopter sling-load simulator for each example with the parameters specified and the control gain as found from figure 11 and equation (8). Figures 14 to 16 are time plots of the thrust of the jets in each axis, the x- and y-coordinates of the control point in each axis, and the velocity and acceleration of the control point in each axis for the uncontrolled load of example 1 and for the controlled loads of the two examples. The uncontrolled motion of the load in example 2 has the same type of characteristics as the uncontrolled load in example 1. In figures 14 to 16, the load is initially displaced 1.2 m in both the x-direction and the y-direction and allowed to swing.

Figure 14 is a time plot without the control system for example 1, and it is seen that the motion of the load is underdamped. The damping seen in figure 14 is from aerodynamic effects. Figure 15 is a time plot with the AJS for example 1 and figure 16 is for example 2.

In example 1 the calculated damping ratio from figure 11 is 0.70, and from figure 15 actual damping ratios of 0.64 in the x-direction and 0.72 in the y-direction are obtained. In example 2, the calculated damping ratio from figure 11 is 0.17, and the actual damping ratios from figure 16 are 0.50 in the x-direction and 0.59 in the y-direction. Aerodynamic forces on the load and nonlinear effects not modeled possibly account for better performance than calculated. Thus, the model used to obtain the control law for this control scheme leads to somewhat conservative results.

Results from variations of the parameters are given in table I. A ±10-percent variation in parameters has the effect of a slight lowering of damping ratio but a slightly larger amount of thrust is required. A -10-percent variation of the parameters results in a higher damping ratio and the same or a slightly smaller amount of thrust. A 10-percent decrease in K_v decreases the damping ratio somewhat and requires less thrust. A 10-percent increase in K_v increases damping ratio but more thrust is required.

A limited number of piloted flights were made with example 1 parameters in hovering, in transition from forward flight at 60 knots to hover, and from hover to forward flight. These were done with the AJS on and off. In the transition from forward flight to hover there was always a significant amount of load swinging as the helicopter came over the landing zone with the AJS off. This swinging caused the pilot to concentrate on reducing the swinging before he could position the load over the landing zone and lower it to the ground. With the AJS on, the load swinging was well damped and this allowed the pilot to concentrate on altitude control and load position control. Load swinging was not a problem in transition from hover to forward flight with the AJS off.

CONCLUSIONS

An active jet control system (AJS) to dampen swinging of a helicopter sling load was studied. The load was modeled as a double pendulum with two degrees of freedom, and small-angle approximations were used in the vertical plane. A velocity feedback control law was developed by using classical root-locus methods. A nondimensional analysis was performed to provide gains for various helicopters, loads, and single-cable suspension systems. The AJS was verified in a full-flight-envelope simulation. The following conclusions were made:

1. Of relative position, velocity, and acceleration feedback, relative velocity feedback provides the highest damping.

2. A ±10-percent change in cable length, sling length, load weight, moment of inertia, and feedback gain affects system performance very slightly.

3. Damping ratios from implementing the AJS in simulation are equal to or greater than 0.7 for the normal range of operating parameters.

4. A limited number of piloted flights in simulation indicate that the AJS significantly dampens load swinging in the transition from forward flight to hover and thus allows the pilot to concentrate on load altitude and position control.

Langley Research Center
National Aeronautics and Space Administration
Hampton, VA 23665
December 6, 1978

APPENDIX

LINEAR MATHEMATICAL MODEL AND POSITION TRANSFER FUNCTION FOR SLING LOAD

The linear mathematical model for the dynamic system shown in figure 2 can be derived by using Lagrange's method. Reference 12 discusses this method and gives (in ch. 2) a set of equations of motion for a double pendulum. The resulting linearized equations of motion for the present system are as follows:

$$I\ddot{\theta} = -\left[x_1 + (\ell_1 + \ell_2)\theta\right] mg \frac{\ell_2}{\ell_1} + F\ell_2 \tag{A1}$$

and

$$m\ddot{x}_1 = -(x_1 + \ell_2\theta)\frac{mg}{\ell_1} + F \tag{A2}$$

Equations (A1) and (A2) are equations (1) and (2), respectively, given in the section "Control Law Development."

Taking the Laplace transform of equation (A1) and solving for $\theta(s)$ gives the following expression:

$$\theta(s) = \frac{X_1(s)\left(-\frac{\ell_2 mg}{\ell_1}\right) + F(s)\ell_2}{Is^2 + (\ell_1 + \ell_2)\frac{\ell_2 mg}{\ell_1}} \tag{A3}$$

Taking the Laplace transform of equation (A2) and solving for $X_1(s)$ gives the following expression:

$$X_1(s) = \frac{\theta(s)\left(-\frac{\ell_2 mg}{\ell_1}\right) + F(s)}{m\left(s^2 + \frac{g}{\ell_1}\right)} \tag{A4}$$

APPENDIX

Substituting equation (A3) for $\theta(s)$ in equation (A4) and solving for $X_1(s)/F(s)$ gives the transfer function for load position as a function of the control force:

$$\frac{X_1(s)}{F(s)} = \frac{\frac{1}{m}\left(s^2 + \frac{\ell_2 mg}{I}\right)}{s^4 + \frac{(\ell_1 + \ell_2)\ell_2 mg + Ig}{I\ell_1} s^2 + \frac{\ell_2 mg^2}{I\ell_1}} \tag{A5}$$

Substituting equation (A4) for $X_1(s)$ in equation (A3) and solving for $\theta(s)/F(s)$ yields the transfer function for attitude as a function of the control force:

$$\frac{\theta(s)}{F(s)} = \frac{\frac{\ell_2}{I} s^2}{s^4 + \frac{(\ell_1 + \ell_2)\ell_2 mg + Ig}{I\ell_1} s^2 + \frac{\ell_2 mg^2}{I\ell_1}} \tag{A6}$$

It is desired to locate the jet thruster at the control point A in figure 2. Therefore, the transfer function $X(s)/F(s)$ must be obtained. This can be accomplished first by using the small-angle approximation

$$x = x_1 + \ell_2\theta \tag{A7}$$

Then, taking the Laplace transform of equation (A7) and putting this into transfer-function form yields

$$\frac{X(s)}{F(s)} = \frac{X_1(s)}{F(s)} + \frac{\ell_2\theta(s)}{F(s)} \tag{A8}$$

Substituting equation (A5) for $X_1(s)/F(s)$ and equation (A6) for $\theta(s)/F(s)$ into equation (A8) gives

APPENDIX

$$\frac{X(s)}{F(s)} = \frac{\frac{I + m\ell_2^2}{Im}\left(s^2 + \frac{\ell_2 mg}{I + m\ell_2^2}\right)}{s^4 + \left[\frac{\ell_2 mg(\ell_1 + \ell_2) + Ig}{I\ell_1}\right]s^2 + \frac{mg^2\ell_2}{I\ell_1}} \tag{A9}$$

Since $I = mk^2$, equation (A9) can be further simplified to yield the load-position transfer function:

$$\frac{X(s)}{F(s)} = \frac{\frac{k^2 + \ell_2^2}{mk^2}\left(s^2 + \frac{\ell_2 g}{k^2 + \ell_2^2}\right)}{s^4 + \frac{\left[\ell_2(\ell_1 + \ell_2) + k^2\right]gs^2}{k^2\ell_1} + \frac{g^2\ell_2}{k^2\ell_1}} = G(s) \tag{A10}$$

which is the same as equation (3) in the section "Control Law Development."

REFERENCES

1. Shaughnessy, J. D.; and Pardue, M. D.: Helicopter Sling Load Accident/Incident Survey: 1968-1974. NASA TM X-74007, 1977.

2. Wolkovitch, Julian; and Johnston, Donald E. (appendices by Claude D. Wezeman, Richard A. Peters, Walter A. Johnson, and Richard P. Walton): Automatic Control Considerations for Helicopters and VTOL Aircraft With and Without Sling Loads. STI Tech. Rep. No. 138-1 (Contract NOw 63-0691), Systems Technology, Inc., Nov. 1965. (Available from DDC as AD 475 537.)

3. Wolkovitch, Julian; Peters, Richard A.; and Johnston, Donald E.: Lateral Control of Hovering Vehicles With and Without Sling Loads. STI Tech. Rep. 145-1 (Contract NOw 64-0407-F), Systems Technology, Inc., May 1966.

4. Gupta, Narendra K.; and Bryson, Arthur E., Jr.: Automatic Control of a Helicopter With a Hanging Load. SUDAAR No. 459, Stanford Univ., Center for Systems Res., June 1973. (Available as NASA CR-136504.)

5. Smith, J. H.; Allen, E. M.; and Vensel, D.: Design, Fabrication, and Flight Test of the Active Arm External Load Stabilization System for Cargo Handling Helicopters. USAAMRDL Tech. Rep. 73-73, U.S. Army, Sept. 1973. (Available from DDC as AD 773 025.)

6. Watkins, T. C.; Sinacori, J. B.; and Kesler, D. F.: Stabilization of Externally Slung Helicopter Loads. USAAMRDL-TR-74-42, U.S. Army, Aug. 1974.

7. Gera, Joseph; and Farmer, Steve W., Jr.: A Method of Automatically Stabilizing Helicopter Sling Loads. NASA TN D-7593, 1974.

8. Asseo, Sabi J.: Feasibility of Using Active Winch Controllers for Sling-Load Stabilization in Heavy Lift Helicopters. Rep. No. TG-3083-J, Cornell Aeronaut. Lab., Inc., Aug. 1971.

9. Garnett, Theodore S., Jr.; and Smith, James H.: Active Arm (External Cargo) Stabilization System Flight Demonstration. USAAMRDL-TR-76-23, U.S. Army, Sept. 1976. (Available from DDC as AD A031 062.)

10. Liu, David T.: In-Flight Stabilization of Externally Slung Helicopter Loads. USAAMRDL Tech. Rep. 73-5, U.S. Army, May 1973.

11. Shaughnessy, J. D.; Deaux, Thomas N.; and Yenni, Kenneth R.: Development and Validation of a Piloted Simulation of a Helicopter and External Sling Load. NASA TP-1285, 1979.

12. Hildebrand, F. B.: Methods of Applied Mathematics. Second ed. Prentice-Hall, Inc., 1965.

TABLE I.- SIMULATION RESULTS

K_v, N-s/m	Parameters (a)	ζ_x	ζ_y	Maximum thrust, N
Example 1				
4069	Given	0.64	0.72	1556
	Given + 10 percent	.63	.68	1645
	Given - 10 percent	.72	.78	1489
3661	Given	0.59	0.63	1489
	Given + 10 percent	.56	.61	1511
	Given - 10 percent	.63	.67	1489
4477	Given	0.78	0.83	1667
	Given + 10 percent	.72	.78	1711
	Given - 10 percent	.83	.85	1645
Example 2				
926	Given	0.50	0.59	1356
	Given + 10 percent	.50	.56	1711
	Given - 10 percent	.53	.59	1356
834	Given	0.50	0.56	1290
	Given + 10 percent	.49	.54	1556
	Given - 10 percent	.56	.56	1290
1019	Given	0.56	0.63	1467
	Given + 10 percent	.50	.59	1845
	Given - 10 percent	.56	.63	1467

[a]Given parameters - Example 1: ℓ_1 = 30.5 m, ℓ_2 = 6.1 m, m = 4536 kg, k^2 = 3.6 m^2. Example 2: ℓ_1 = 6.1 m, ℓ_2 = 6.1 m, m = 454 kg, k^2 = 6.2 m^2.

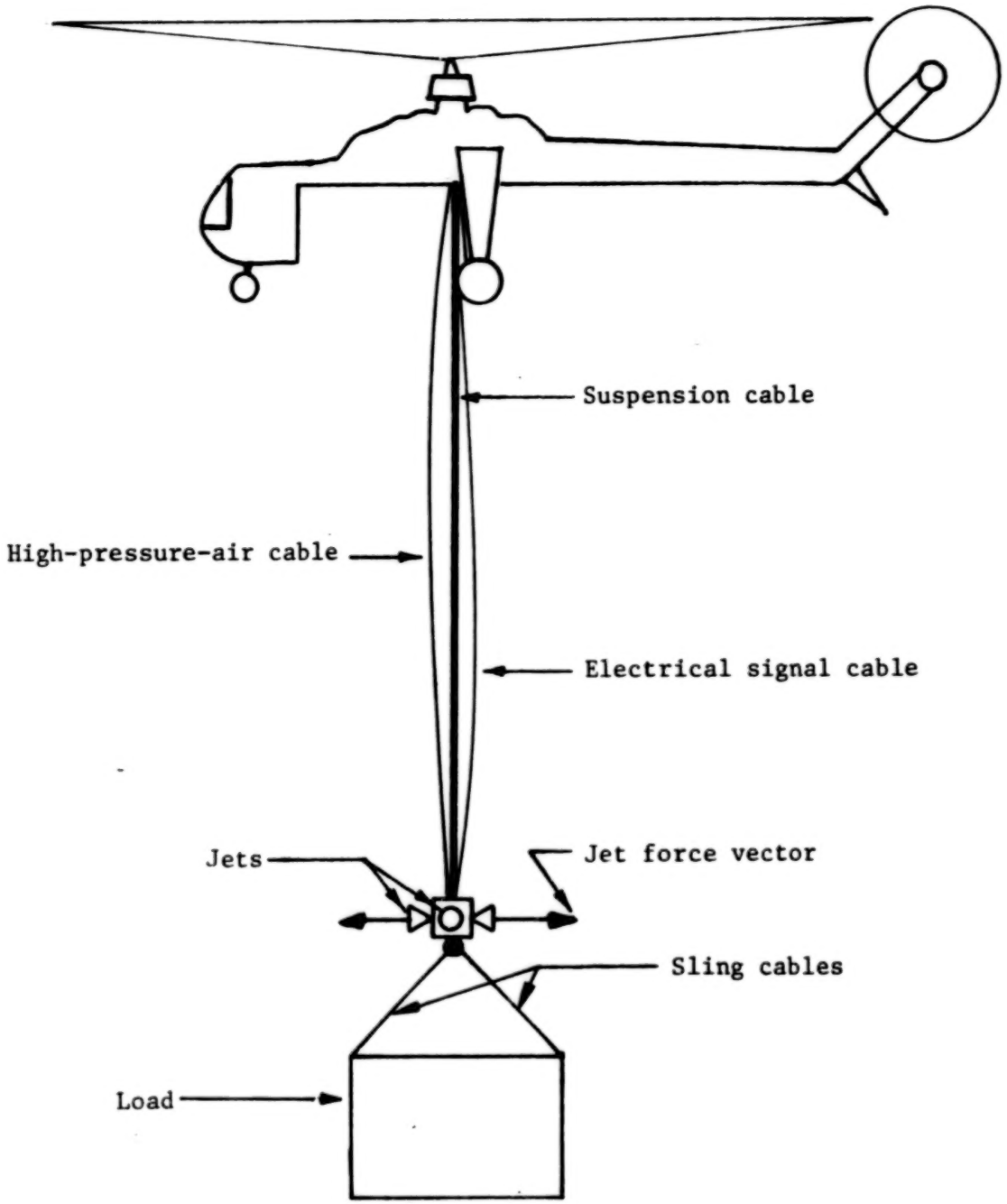

Figure 1.- Active jet control system scheme.

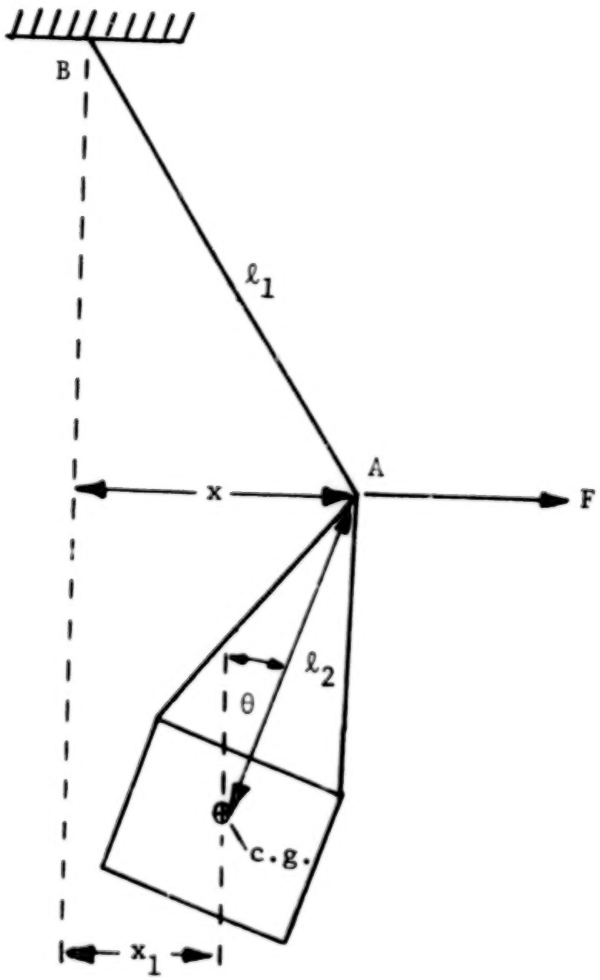

Figure 2.- Double-pendulum model of a sling load.

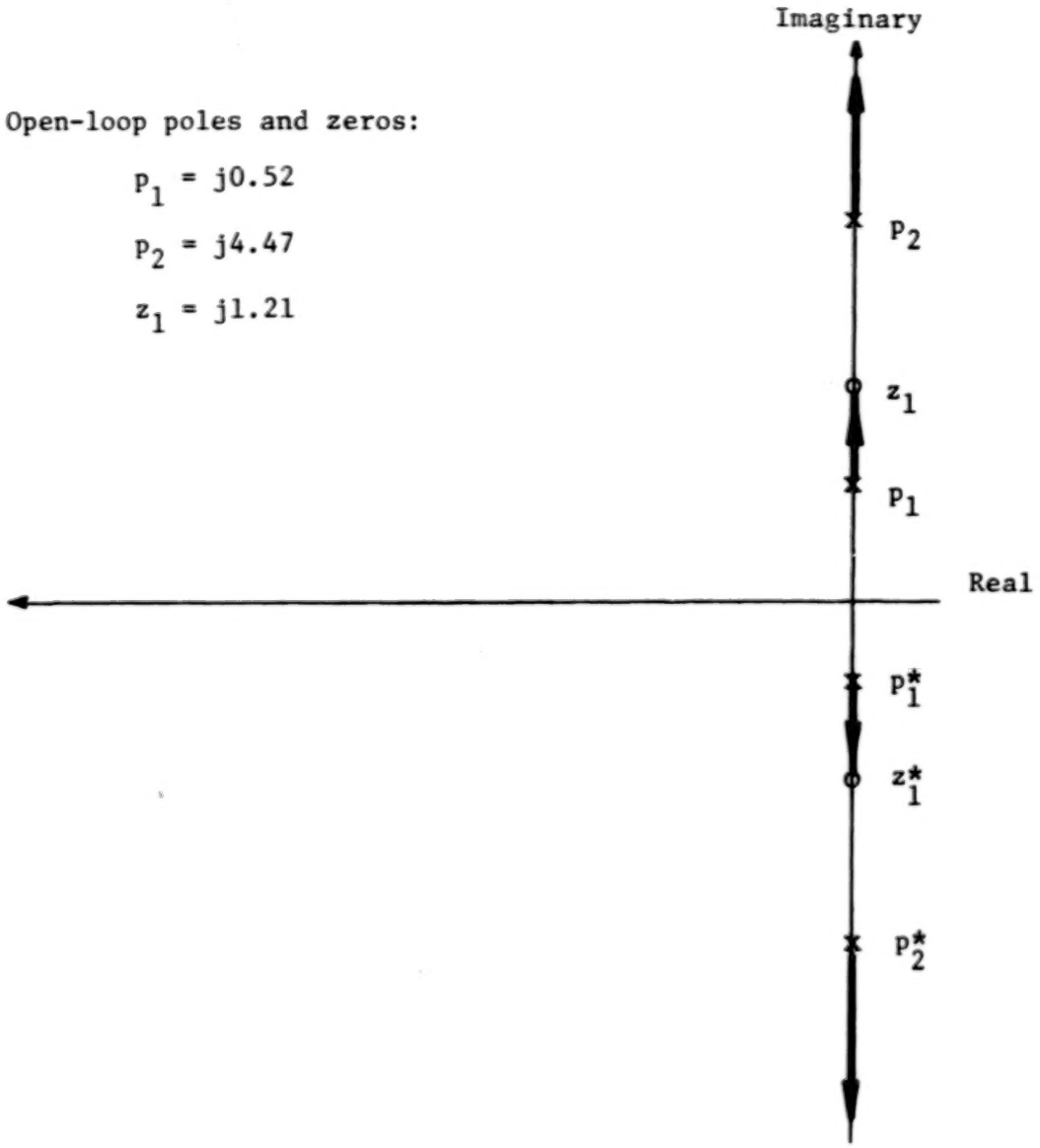

Figure 3.- Root locus of position feedback control system with $K_p \geq 0$ for $\ell_1 = 30.5$ m, $\ell_2 = 6.1$ m, $m = 4536$ kg, and $k^2 = 3.6$ m^2.

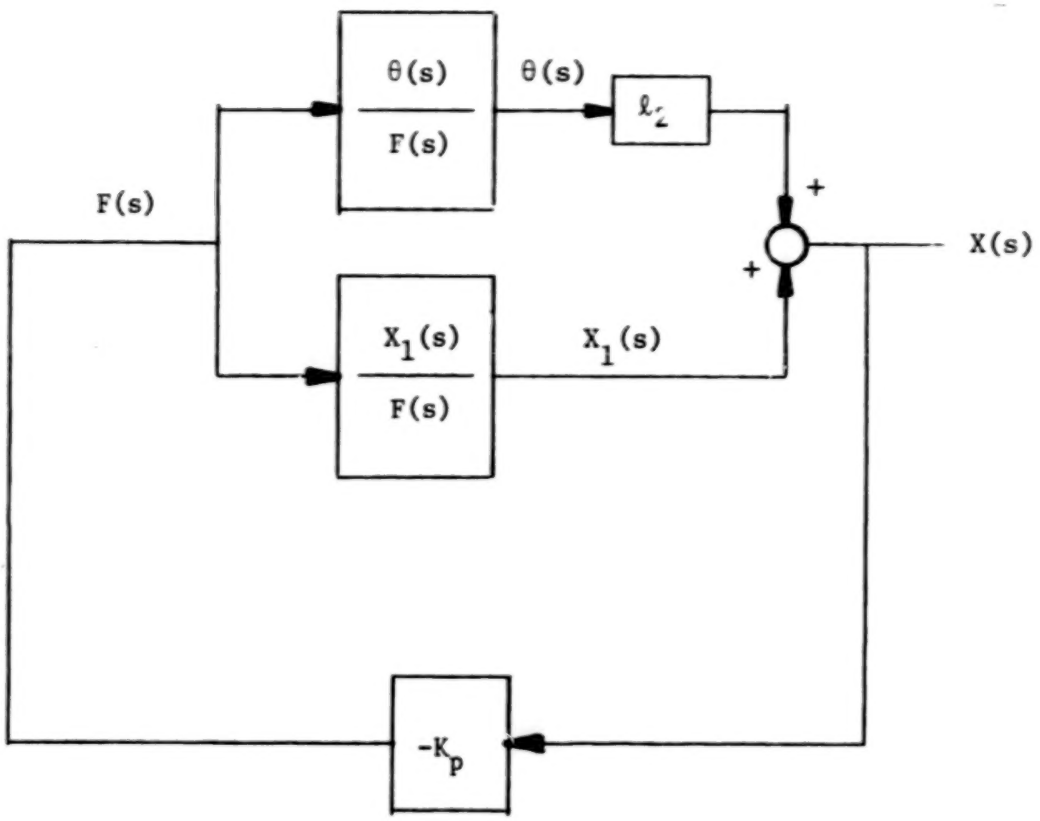

Figure 4.- Block diagram of position feedback control system.

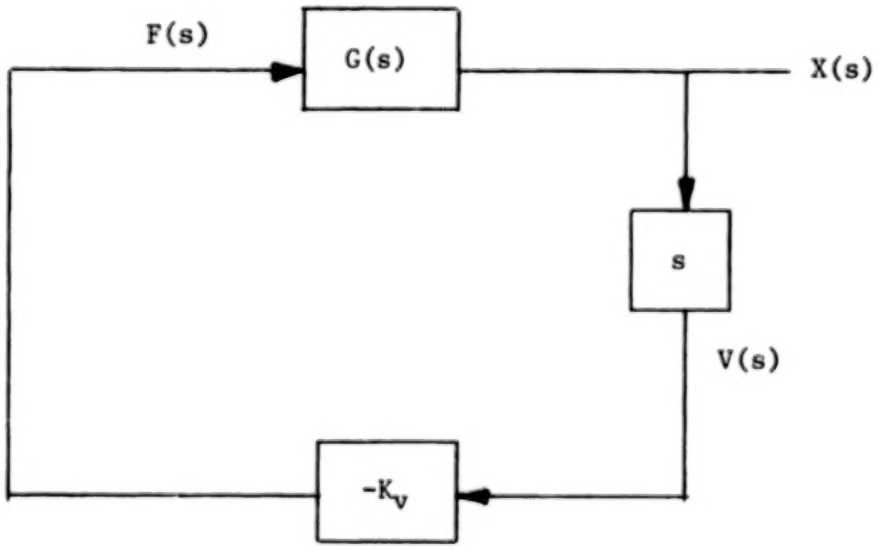

Figure 5.- Block diagram of velocity feedback control system.

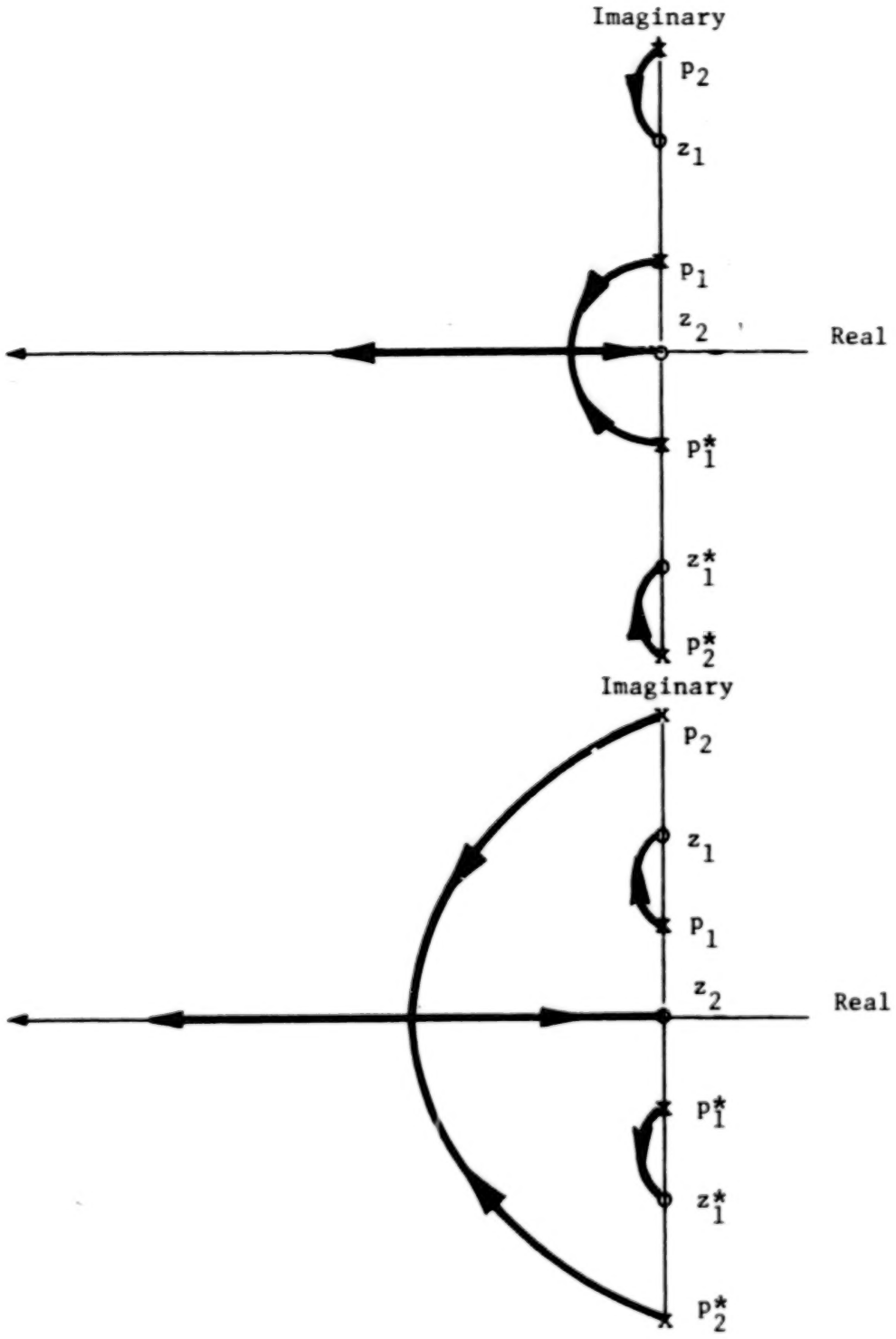

Figure 6.- Two possible root loci of velocity feedback control system with $K_v > 0$.

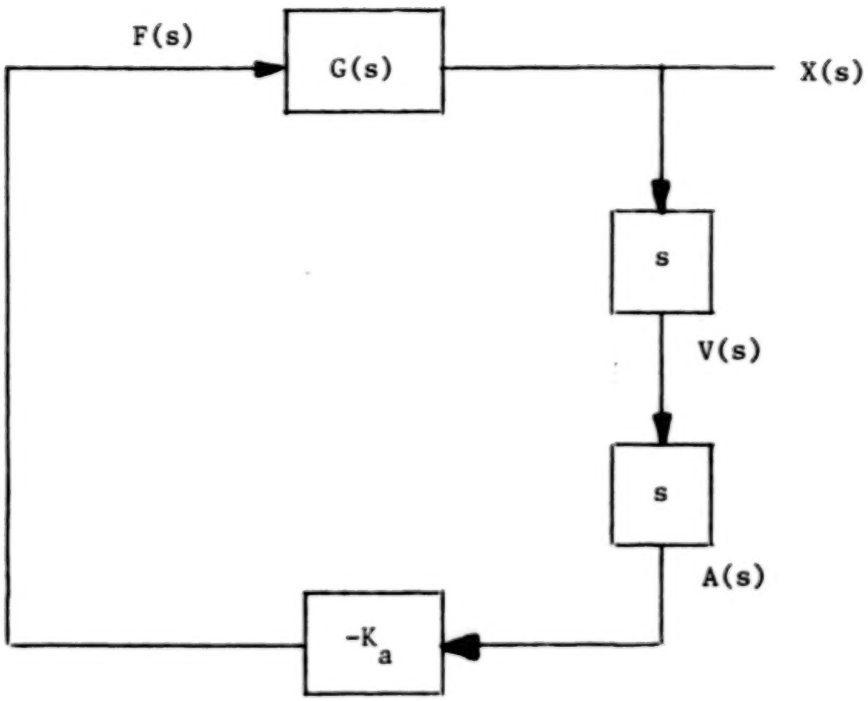

Figure 7.- Block diagram of acceleration feedback control system.

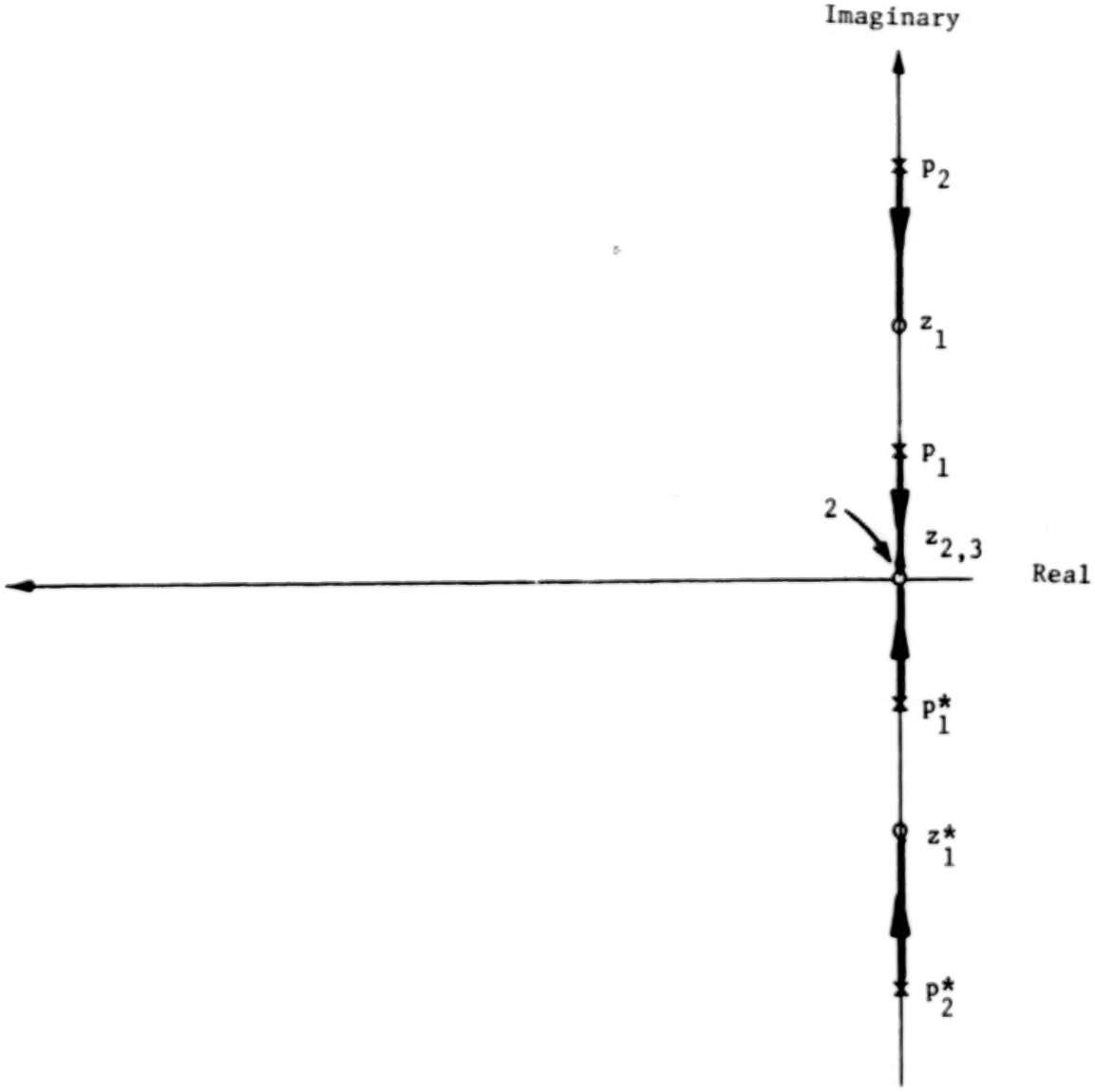

Figure 8.- Root locus of acceleration feedback control system with $K_a > 0$.

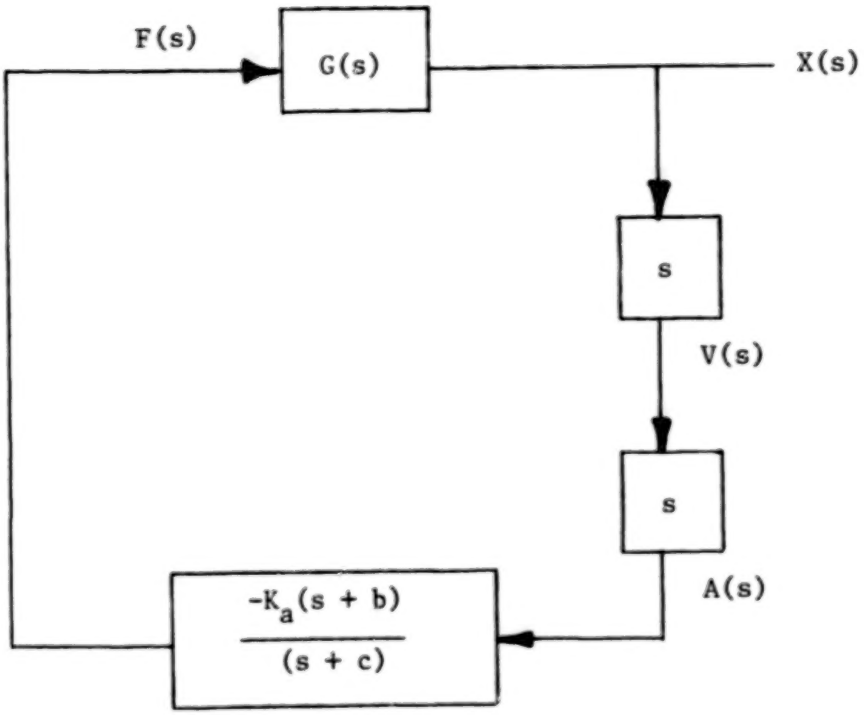

Figure 9.- Block diagram of acceleration feedback control system with a cascade lead compensator in the feedback loop.

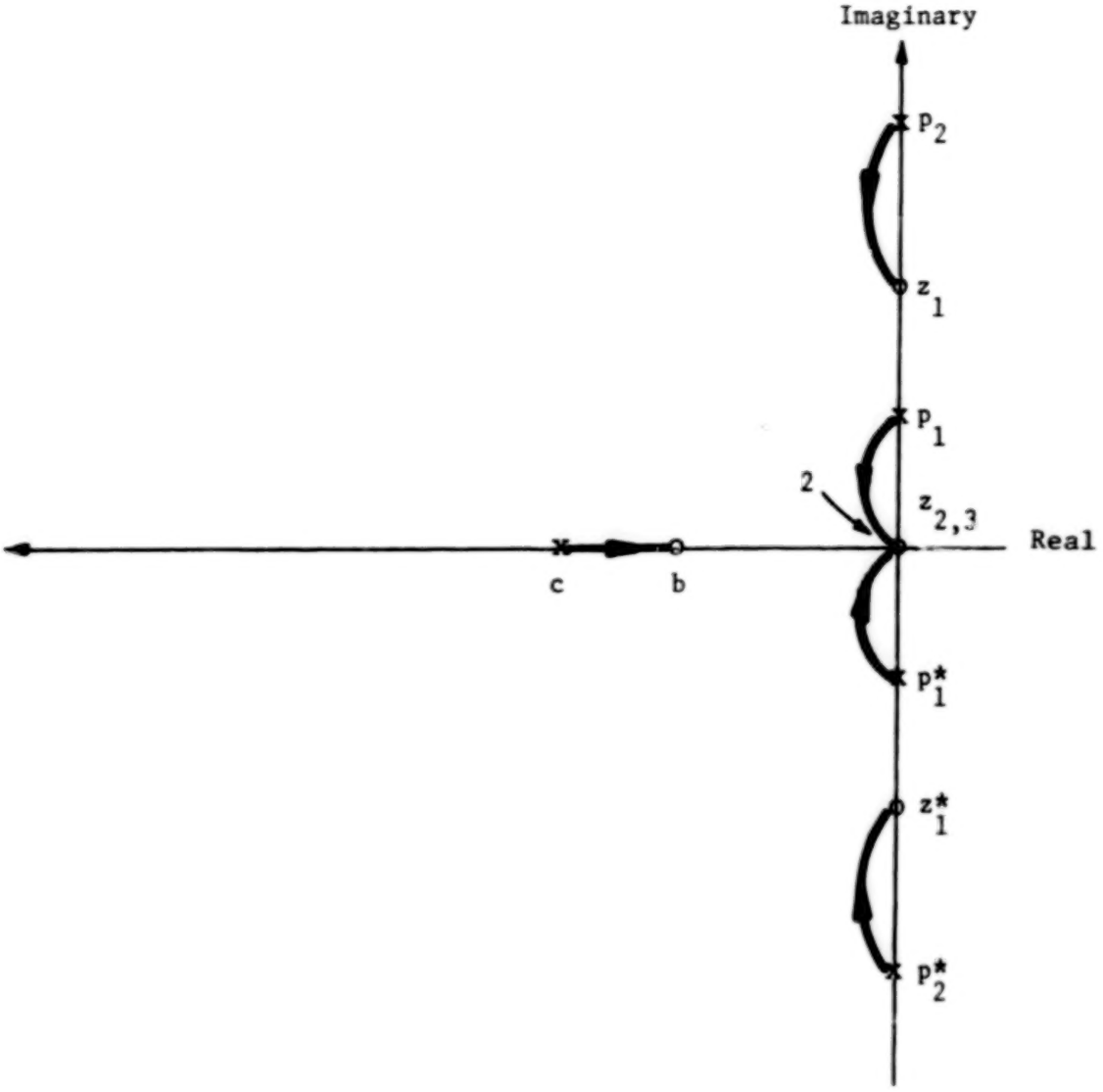

Figure 10.- Root locus of the control system shown in figure 9 with $K_a > 0$.

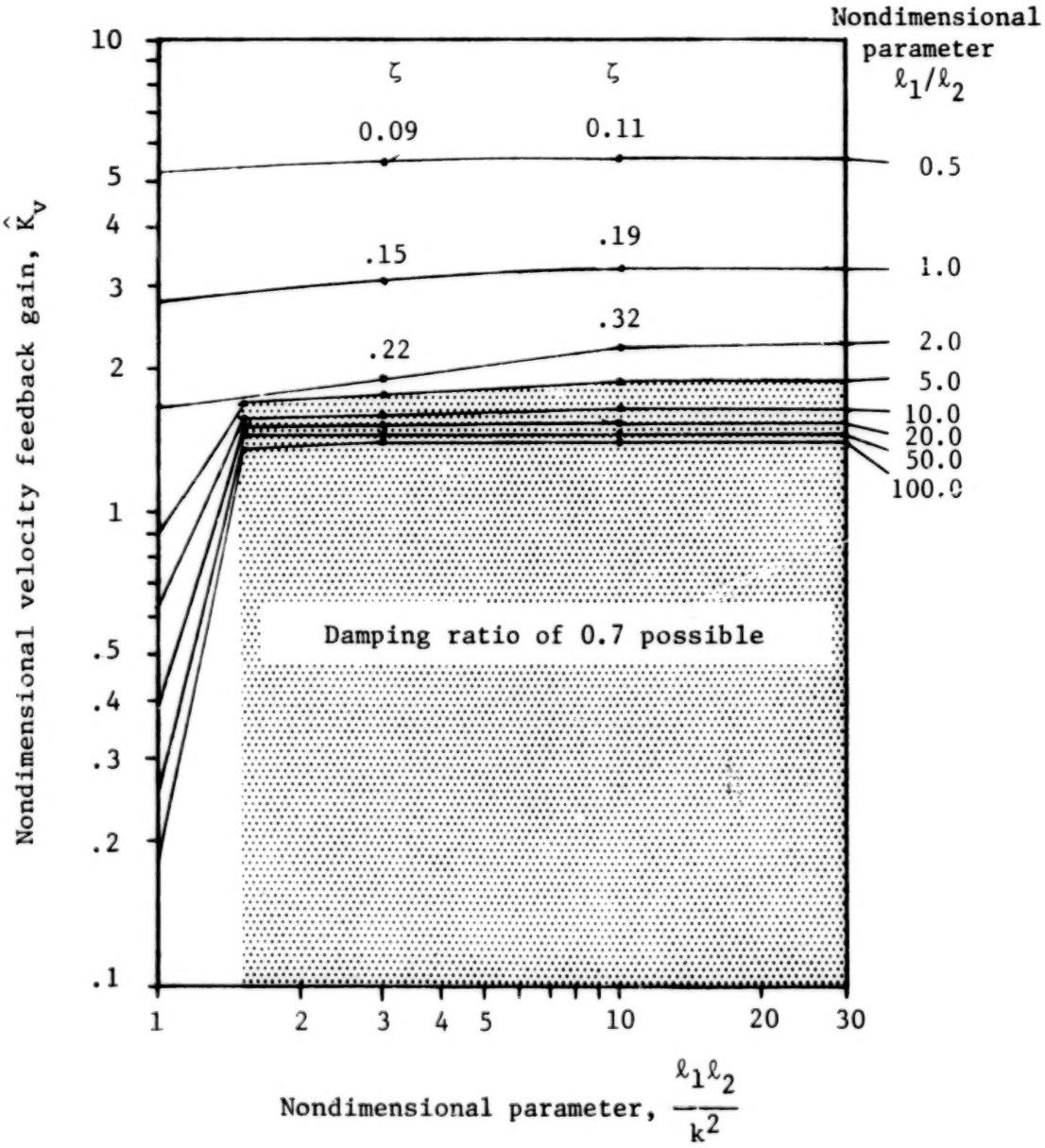

Figure 11.- Nondimensional velocity feedback gain $\hat{K}_v$ versus $\ell_1\ell_2/k^2$ for different values of ℓ_1/ℓ_2.

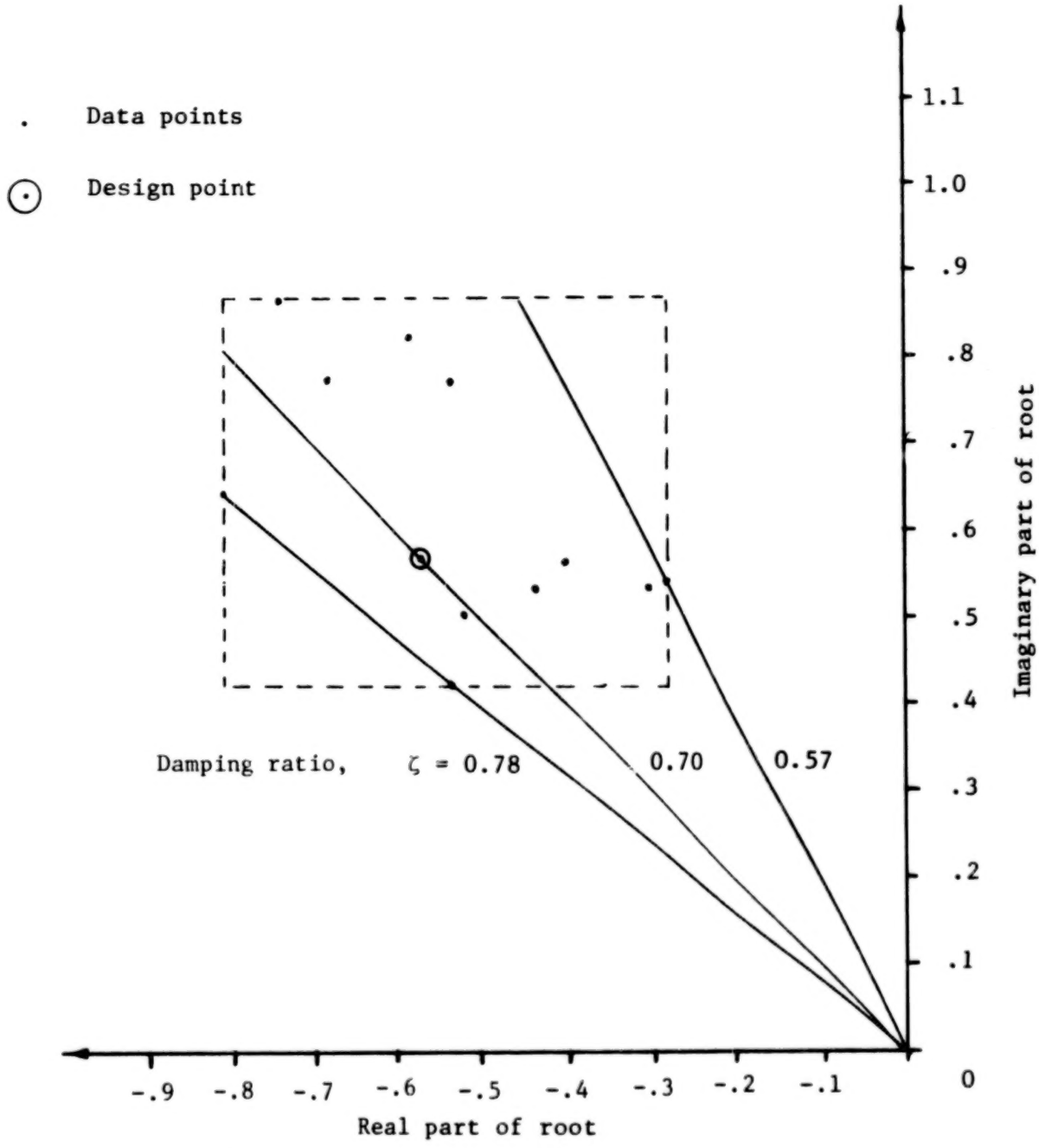

Figure 12.- Calculated migration of pendulum-mode roots for a ±10-percent variation in parameters. ℓ_1 = 30.5 m; ℓ_2 = 6.1 m; k^2 = 3.6 m^2; m = 4536 kg.

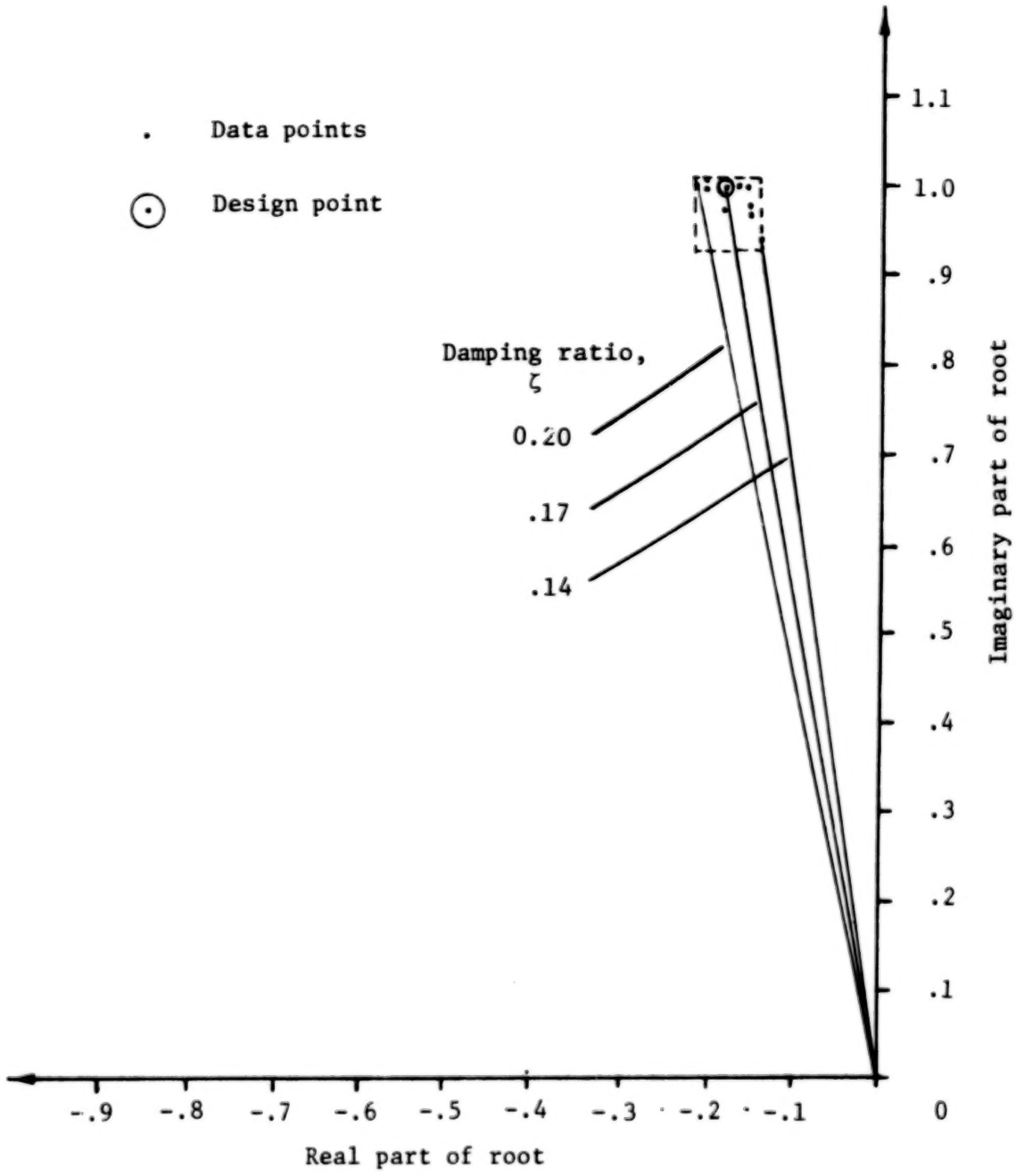

Figure 13.- Calculated migration of pendulum-mode roots for a ±10-percent variation in parameters. $\ell_1 = \ell_2 = 6.1$ m; $k^2 = 6.2$ m^2; m = 454 kg.

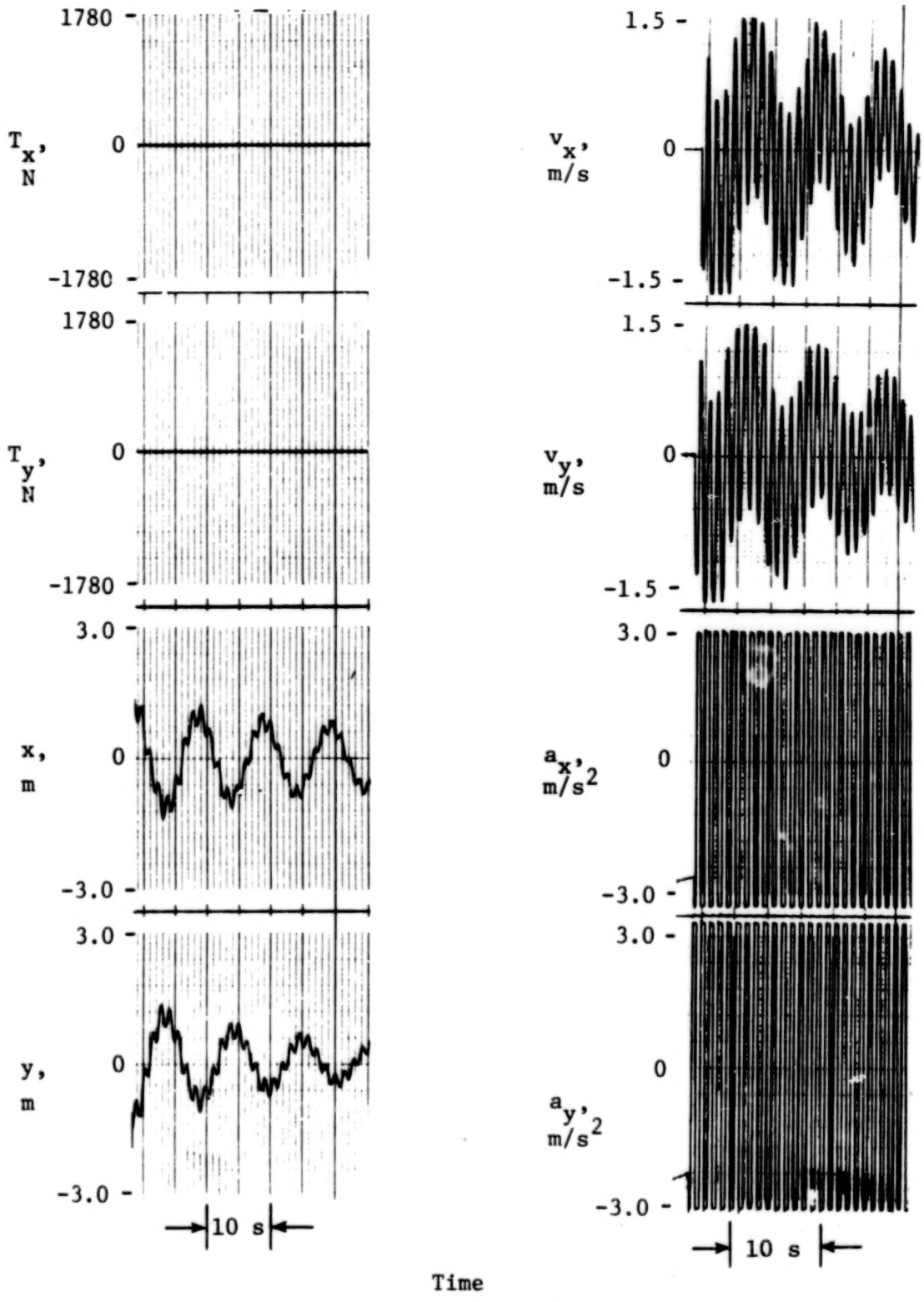

Figure 14.- Uncontrolled load motion for example 1.

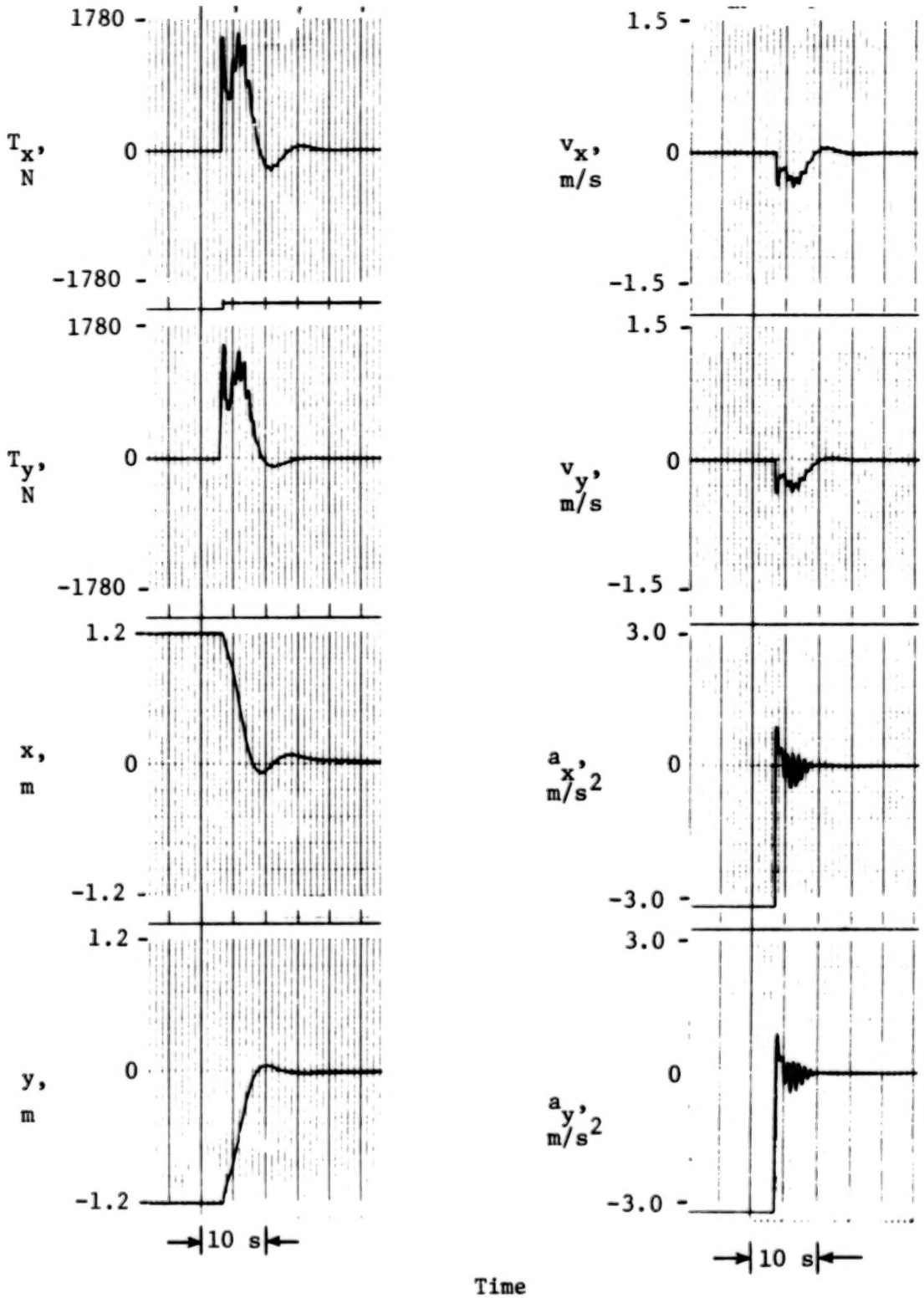

Figure 15.- Example 1: K_v = 4069 N-s/m.

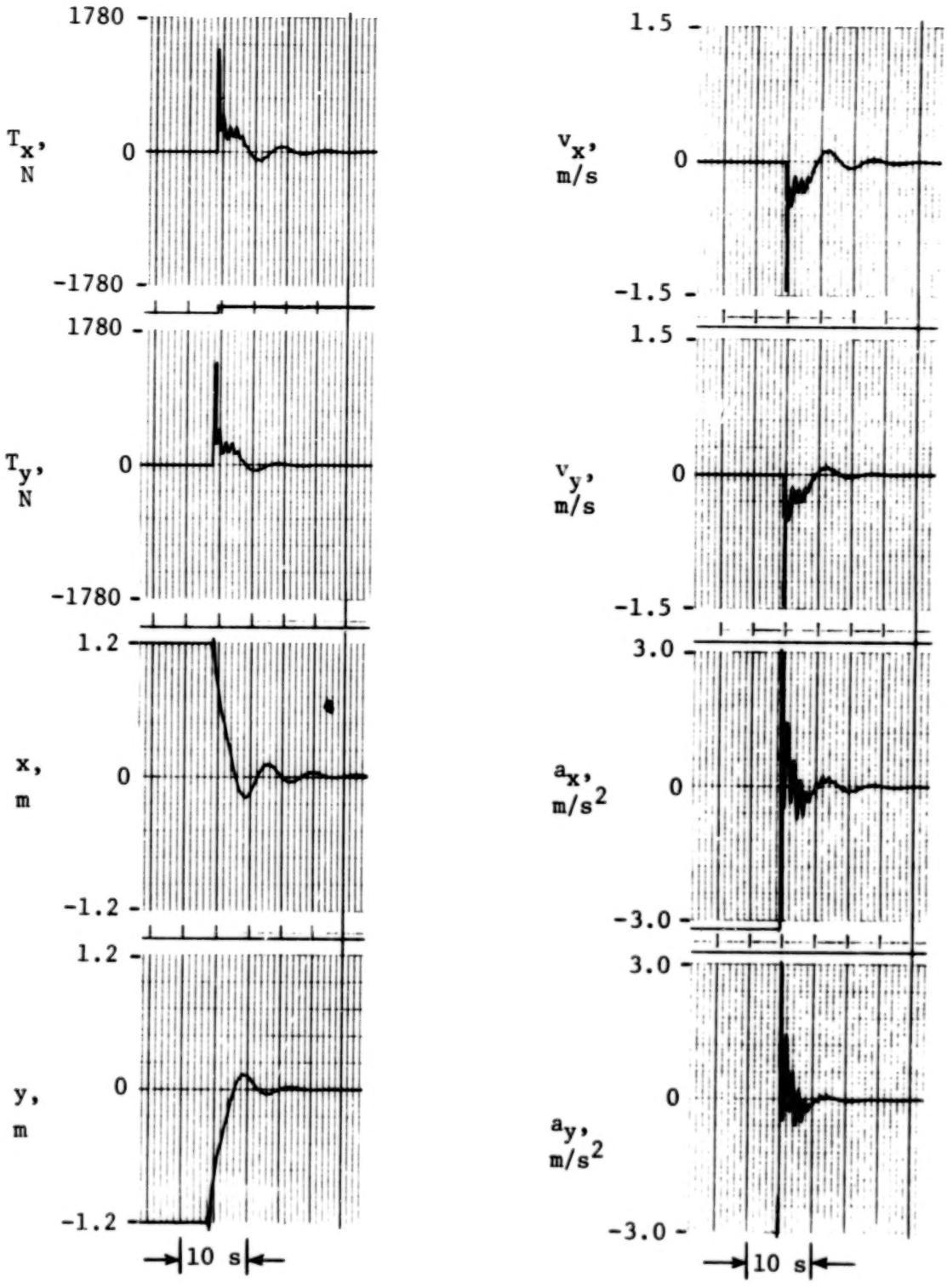

Figure 16.- Example 2: K_v = 926 N-s/m.

1. Report No.	2. Government Accession No.	3. Recipient's Catalog No.
NASA TP-1397		

4. Title and Subtitle	5. Report Date
DESIGN AND ANALYSIS OF AN ACTIVE JET CONTROL SYSTEM FOR HELICOPTER SLING LOADS	January 1979
	6. Performing Organization Code
7. Author(s)	8. Performing Organization Report No.
Mark D. Pardue and J. D. Shaughnessy	L-11836
	10. Work Unit No.
9. Performing Organization Name and Address	505-09-53-01
NASA Langley Research Center Hampton, VA 23665	11. Contract or Grant No.
	13. Type of Report and Period Covered
12. Sponsoring Agency Name and Address	Technical Paper
National Aeronautics and Space Administration Washington, DC 20546	14. Sponsoring Agency Code

15. Supplementary Notes

Mark D. Pardue: Old Dominion University, Norfolk, Virginia.
J. D. Shaughnessy: Langley Research Center.

The information in this paper is largely based on a thesis submitted by Mark D. Pardue in partial fulfillment of the requirements for the degree of Master of Engineering, Old Dominion University, Norfolk, Virginia, May 1977.

16. Abstract

An active jet control system for stabilizing the swinging motion of helicopter external sling loads in hover (and forward flight) is described. A velocity feedback control law is obtained by using classical control theory. A nondimensional analysis is performed to give a simple chart for determining the appropriate value of feedback gain as a function of cable length, sling length, and load parameters to provide theoretical damping ratios of 0.7. The sensitivity to parameter changes was studied, and a ±10-percent change in parameters was found to affect system performance only slightly. Implementation of the control scheme in a nonlinear simulation produced damping ratios equal to or greater than those calculated. A limited number of piloted flights in a visual simulator indicated a significant reduction in load swinging in the transition to hover, and thus the pilot was able to concentrate on load altitude and position control.

17. Key Words (Suggested by Author(s))	18. Distribution Statement
Helicopters External sling loads Automatic control system analysis	Unclassified - Unlimited Subject Category 08

19. Security Classif. (of this report)	20. Security Classif. (of this page)	21. No. of Pages	22. Price*
Unclassified	Unclassified	32	$4.50

* For sale by the National Technical Information Service, Springfield, Virginia 22161

NASA-Langley, 1979

END

APR 30 1979